Mark J. Jackson · Jonathan S. Morrell
Editors

Machining with Nanomaterials

Second Edition

Springer

Machining with Nanomaterials

Mark J. Jackson • Jonathan S. Morrell
Editors

Machining with Nanomaterials

Second Edition

Springer

Editors
Mark J. Jackson
Micro Machinists Group
Cambridge, MA, USA

Jonathan S. Morrell
Compatibility and Surveillance Section
Y-12 National Security Complex
Oak Ridge, TN, USA

ISBN 978-3-319-19008-2 ISBN 978-3-319-19009-9 (eBook)
DOI 10.1007/978-3-319-19009-9

Library of Congress Control Number: 2015944197

Springer Cham Heidelberg New York Dordrecht London

Printed on acid-free paper

Springer International Publishing AG Switzerland is part of Springer Science+Business Media (www.springer.com)

Preface

Machining is a widely used process for producing intricate shapes on components and artifacts and for providing precise tolerances that are required for the manufacture of parts at the micro- and nanoscale. Modern machining requires the use of minimum quantities of lubricants, dry machining capability, high cutting speeds, and long tool lives. However, existing tool materials have proven to be substandard compared to newly developed nanostructured thin film coated cutting tools. There is also a growing need for specially developed cutting tools for machining high strength and hardness nanocrystalline metals and alloys.

In January 2000, President William J. Clinton talked about the exciting promise of nanotechnology and later announced an ambitious national nanotechnology initiative (NNI) that was enacted in 2001, and reauthorized by President George W. Bush in 2006, with an initial budget of $497 million to promote nanoscale research that would benefit society. The initiative has created a new industry focused on providing nanostructured coatings and materials. The purpose of this book is to present information and knowledge on the rapidly developing field of machining with nanomaterials. The book is written in the spirit of scientific endeavor outlined by Richard Feynman, who stated in 1960 that one of the greatest challenges to scientists in the field of miniaturization is the manufacture of objects using techniques such as turning and milling. The second edition of this book presents information on machining fundamentals, machining stability and chatter, developments in tool coatings, machining common engineering materials with coated tools, dry machining, creating nanostructured metals using coated cutting tools, multi-optimization of cutting conditions using coated tools, machining with recoated cutting tools, modeling and machining biomaterials, and machining with nanostructured abrasive diamond.

The structure of the book is based on matter provided by many colleagues and the author wishes to thank the contributors of this book for helping construct a source of knowledge and database on machining with nanomaterials and for

granting the editors permission to use such material. The editors also acknowledge the help and support of Inderscience and Springer Publishers for allowing the chapter contributors and editors to reproduce their work that was originally published in refereed Inderscience journals and Springer publications.

Cambridge, MA, USA Mark J. Jackson
Oak Ridge, TN, USA Jonathan S. Morrell
March 2015

Contents

About the Editors

Mark J. Jackson began his engineering career in 1983 when he studied for his O.N.C. part I examinations and his first-year apprenticeship training course in mechanical engineering. After gaining his Ordinary National Diploma in Engineering with distinctions and I.C.I. prize for achievement, he read for a degree in mechanical and manufacturing engineering at Liverpool Polytechnic and spent periods in industry working for I.C.I. Pharmaceuticals, Unilever Industries, Rolls-Royce, and Anglo Blackwells. After graduating with a Master of Engineering (M.E.) degree with Distinction under the supervision of Professor Jack Schofield, M.B.E., Dr. Jackson subsequently read for a Doctor of Philosophy (Ph.D.) degree at Liverpool in the field of materials engineering focusing primarily on microstructure–property relationships in vitreous-bonded abrasive materials under the supervision of Professor Benjamin Mills. He was subsequently employed by Unicorn Abrasives' Central Research & Development Laboratory (Saint-Gobain Abrasives' Group) as materials technologist, then technical manager, responsible for product and new business development in Europe, and university liaison projects concerned with abrasive process development. Dr. Jackson then became a research fellow at the Cavendish Laboratory, University of Cambridge, working with Professor John Field, O.B.E., F.R.S., on impact fracture and friction of diamond before becoming a lecturer in engineering at the University of Liverpool in 1998. At Liverpool, Dr. Jackson established research in the field of micromachining using mechanical tools, laser beams, and abrasive particles. At Liverpool, he attracted a number of research grants concerned with developing innovative manufacturing processes for which he was jointly awarded an Innovative Manufacturing Technology Center from the Engineering and Physical Sciences Research Council in November 2001. In 2002, he became associate professor of mechanical engineering and faculty associate in the Center for Manufacturing Research, and Center for Electric

Power at Tennessee Technological University (an associated university of Oak Ridge National Laboratory), and a faculty associate at Oak Ridge National Laboratory. Dr. Jackson was the academic adviser to the Formula SAE Team at Tennessee Technological University. In 2004, he moved to Purdue University as Professor of Mechanical Engineering in the College of Technology and served at the Benjamin Franklin Institute of Technology as Department Chairman of the Mechanical Engineering Department. In 2013, Dr. Jackson became the McCune and Middlekauff Foundation Endowed Faculty Fellow and Academic Department Head at Kansas State University.

Dr. Jackson is active in research work concerned with understanding the properties of materials in the field of microscale metal cutting, micro- and nano-abrasive machining, and laser micromachining. He is also involved in developing next generation manufacturing processes. Dr. Jackson has directed, co-directed, and managed research grants funded by the Medical Research Council, Engineering and Physical Sciences Research Council, The Royal Society of London, The Royal Academy of Engineering (London), European Union, Ministry of Defense (London), Atomic Weapons Research Establishment, National Science Foundation, N.A.S.A., U.S. Department of Energy (through Oak Ridge National Laboratory), Y-12 National Security Complex at Oak Ridge, Tennessee, and Industrial Companies, which has generated research income in excess of $15 million. Dr. Jackson has organized many conferences and served as General Chairman of the International Surface Engineering Congress and is Deputy President of the World Academy of Materials and Manufacturing Engineering. He has authored and coauthored over 250 publications in archived journals and refereed conference proceedings, and has written and edited books in the area of nanotechnology and manufacturing.

Jonathan S. Morrell a senior chemist and technical manager at the Y-12 National Security Complex in Oak Ridge, Tennessee, and has led the Compatibility and Surveillance Section of the Development Division since 2005. As a technical manager, Dr. Morrell oversees projects related to nuclear programs supporting core surveillance with nondestructive, destructive, and component testing. This involves testing of nuclear reactor fuels, cladding, and structural materials for performance evaluation, as well as long-term compatibility issues. Further, he conducts fundamental studies of material property variations and performance due to the direct effects of environment-induced degradation in the presence of temperature gradients, mechanical stresses, reactive and moist ambiances, and chemical and radioactive conditions for national security applications. Dr. Morrell currently serves on several coordinated research projects at the International Atomic Energy Agency (IAEA) in Vienna, Austria on lifetime extension of aging research reactors. He is also an adjunct faculty professor in the Department of Chemistry at the University of

Tennessee and in the Natural and Behavioral Science Department at Pellissippi State Community College in Knoxville. Dr. Morrell has 10 issued patents, authored and coauthored more than 32 publications in archived journals and refereed conference proceedings, authored over 110 formal reports, and edited 4 technical books. He is currently a member of the editorial boards of the *International Journal of Molecular Engineering*, *International Journal of Nano and Biomaterials*, and *International Journal of Nanoparticles*.

Dr. Morrell received his bachelor degrees with honors from King College in chemistry and in biology. His honors research was conducted at the J. H. Quillen College of Medicine on the campus of East Tennessee State University, Johnson City, Tennessee, and was funded under a grant from the Department of Biochemistry and Molecular Biology at John Hopkins Medical Institute. The topic of this research was the antibiotic inhibition of ribosomal subunit formation in *Escherichia coli* cells. His doctor of philosophy in inorganic chemistry was obtained in 2000 from the University of Tennessee in Knoxville under the guidance of Professors David B. Beach and Ziling B. Xue. For his doctoral dissertation, Dr. Morrell studied the heteroepitaxial growth of complex oxide thin films via solution chemical techniques using novel alkoxide precursors. This research involved both the synthesis of precursor solutions and the processing and characterization of epitaxial thin films for ferroelectric and superconductor applications. The research was conducted at the Oak Ridge National Laboratory (ORNL), Oak Ridge, Tennessee, under a grant from the Office of Basic Energy Sciences, United States Department of Energy. Dr. Morrell, briefly employed by ORNL as a postdoctoral fellow, joined the Y-12 National Security Complex, Oak Ridge, Tennessee, in the summer of 2000. As a principal investigator in the Development Division, he was involved in experimental testing and small-scale verification of operating conditions associated with industrial production issues related to national defense. Dr. Morrell later initiated research and development programs in pyrochemistry, materials processing, forensic analysis, machining, sintering and densification studies on IAEA reactor fuels, and environmental aging studies. Dr. Morrell currently resides in his native home of East Tennessee with his twin sons, Graham and Parker.

Chapter 1
Fundamentals of Machining

Mark J. Jackson, M.D. Whitfield, G.M. Robinson, R.G. Handy, Jonathan S. Morrell, J.P. Davim, W. Ahmed, and H. Sein

Abstract During chip formation there is a substantial increase in the specific energy as chip size is reduced during machining. It is believed this is due to the fact that all metals contain defects such as grain boundaries, missing and impurity atoms, and when the size of the material removed decreases the probability of encountering a stress-reducing defect decreases. Since the shear stress and strain in metal cutting is unusually high, discontinuous microcracks usually form on the primary shear plane. If the material is very brittle, or the compressive stress on the shear plane is relatively low, microcracks will grow into larger cracks giving rise to discontinuous chip formation. When discontinuous microcracks form on the shear plane they will weld and reform as strain proceeds, thus joining the transport of dislocations in accounting for the total slip of the shear plane. This chapter focuses on machining at the micro- and nanoscale and attempts to explain the dominant features of machining as the size effect becomes significant.

Keywords Machining • Size effects • Nanomachining • Micromachining • Nanomaterials

1.1 Introduction: Machining Effects

It has been known for a long time that a size effect exists in metal cutting, where the specific energy increases with decrease in deformation size. Figure 1.1 shows the construction of a tool moving into a piece of metal at a certain speed to form a pronounced chip and the associated deformation zone showing the nature of flow

M.J. Jackson (✉) • M.D. Whitfield • G.M. Robinson • R.G. Handy
Micro Machinists Group, Cambridge, MA, USA
e-mail: bondedabrasive@gmail.com

J.S. Morrell
Y12-National Security Complex, Oak Ridge, TN, USA

J.P. Davim
University of Aveiro, Aveiro, Portugal

W. Ahmed • H. Sein
University of Central Lancashire, Preston, UK

M.J. Jackson, J.S. Morrell (eds.), *Machining with Nanomaterials*,
DOI 10.1007/978-3-319-19009-9_1

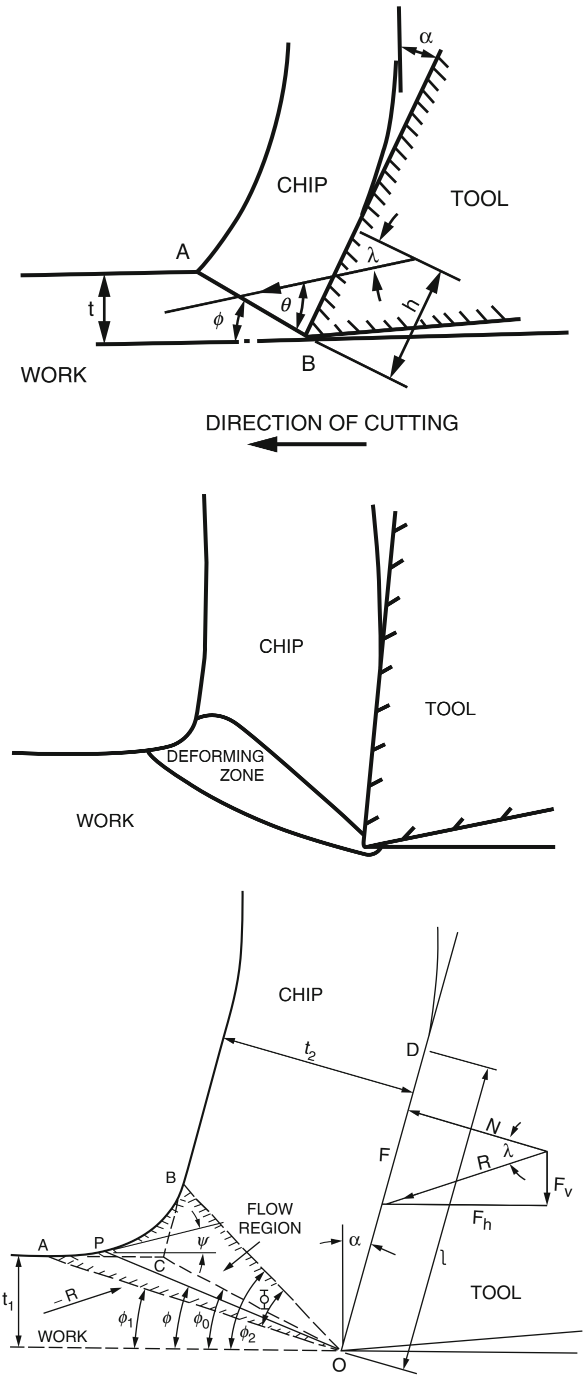

Fig. 1.1 Chip formation relationships when cutting with no built-up edge [1]

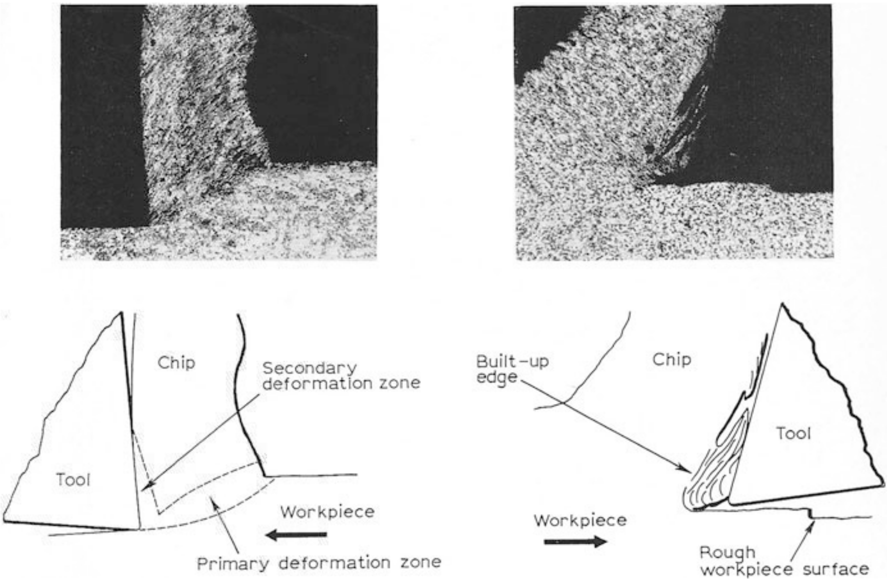

Fig. 1.2 Metal cutting with a built-up edge [1]

and its relationship to various machining parameters. Figure 1.2 shows the nature of cutting with a built-up edge. Backer et al. [1] performed a series of experiments in which the shear energy per unit volume deformed (u_S) was determined as a function of specimen size for a ductile metal (SAE 1112 steel). The deformation processes involved were as follows, listed from top to bottom with increasing size of specimen deformed:

- Surface grinding
- Micromilling
- Turning
- Tensile testing

The surface grinding experiments were performed under relatively mild conditions involving plunge type experiments in which an 8-in. (20.3 cm) diameter wheel was directed radially downward against a square specimen of length and width 0.5 in. (1.27 cm). The width of the wheel was sufficient to grind the entire surface of the work at different downfeed rates (t). The vertical and horizontal forces were measured by a dynamometer supporting the workpiece. This enabled the specific energy (u_S) and the shear stress on the shear plane (τ) to be obtained for different values of undeformed chip thickness (t). The points corresponding to a constant specific energy below a value of down feed of about 28 μin. (0.7 μm) are on a horizontal line due to a constant theoretical strength of the material being reached when the value of t goes below approximately 28 μin. (0.7 μm). The reasoning in support of this conclusion is presented in Backer et al. [1].

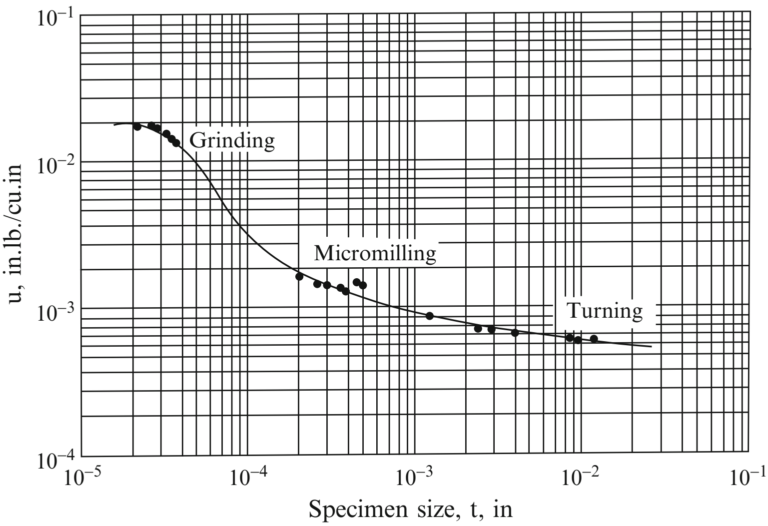

Fig. 1.3 Variation of shear stress on shear plane when cutting SAE 1112 steel [1]

In the micromilling experiments, a carefully balanced 6-in. (152 cm) carbide tipped milling cutter was used with all but one of the teeth relieved so that it operated as a fly milling cutter. Horizontal and vertical forces were measured for a number of depths of cut (t) when machining the same sized surface as in grinding. The shear stress on the shear plane (τ) was estimated by a rather detailed method presented in Backer et al. [1]. Turning experiments were performed on a 2.25-in. (5.72 cm) diameter SAE 1112 steel bar pre-machined in the form of a thin-walled tube having a wall thickness of 0.2 in. (5 mm). A zero degree rake angle carbide tool was operated in a steady-state two-dimensional orthogonal cutting mode as it machined the end of the tube. Values of shear stress on the shear plane (τ) versus undeformed chip thickness were determined for experiments at a constant cutting speed and different values of axial infeed rate and for variable cutting speeds and a constant axial infeed rate. The grinding, micromilling, and turning results are shown in Fig. 1.3.

A true stress–strain tensile test was performed on a 0.505-in. (1.28 cm) diameter by 2-in. (5.08 cm) gage length specimen of SAE 1112 steel. The mean shear stress at fracture was 22,000 psi (151.7 MPa). This value is not shown in Fig. 1.1 since it falls too far to the right. Taniguchi discussed the size effect in cutting and forming and presented his version of Fig. 1.1 in Fig. 1.4 [2]. Shaw [3] discusses the origin of the size effect in metal cutting, which is believed to be primarily due to short-range inhomogeneities present in all engineering metals.

When the back of a metal cutting chip is examined at very high magnification by means of an electron microscope individual slip lines are evident as shown in Fig. 1.5. In deformation studies, Heidenreich and Shockley [4] found that slip does not occur on all atomic planes but only on certain discrete planes. In experiments on deformed aluminum single crystals the minimum spacing of adjacent slip

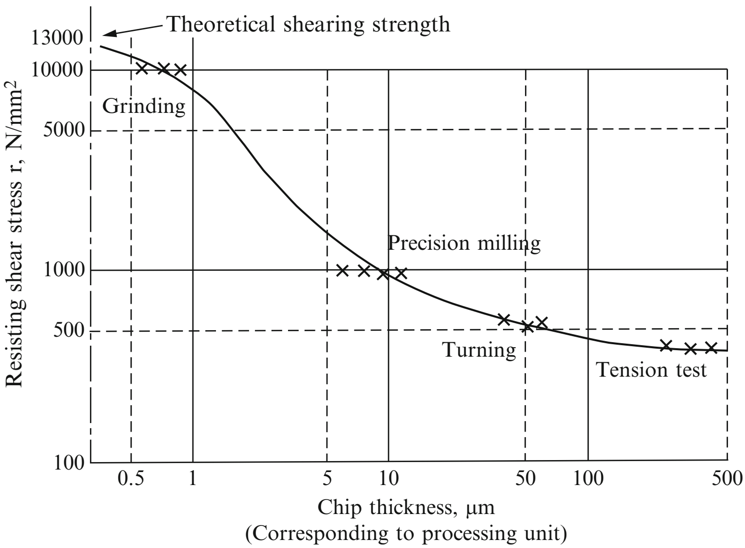

Fig. 1.4 Relationship between chip thickness and resisting shear stress for Fig. 1.3 as modified by Taniguchi [2]

planes was found to be approximately 50 atomic spaces while the mean slip distance along the active slip planes was found to be about 500 atomic spaces. These experiments further support the observation that metals are not homogeneous and suggest that the planes along which slip occurs are associated with inhomogeneities in the metal. Strain is not uniformly distributed in many cases. For example, the size effect in a tensile test is usually observed only for specimens less than 0.1 in. (2.5 mm) in diameter. On the other hand, a size effect in a torsion test occurs for considerably larger samples due to the greater stress gradient present in a torsion test than in a tensile test. This effect and several other related ones are discussed in detail by Shaw [3].

1.1.1 Prediction of friction power Angle

There have been many notable attempts to derive an equation for the shear angle (ϕ) shown in Fig. 1.6 for steady-state orthogonal cutting. Ernst and Merchant [5] presented the first quantitative analysis. Figure 1.7 shows forces acting on a chip at the tool point where $R =$ the resultant force on the tool face, $R' =$ the resultant force in the shear plane, N_C and F_C are the components of R normal to and parallel to the tool face, N_S and F_S are the components of R' normal to and parallel to the cutting direction, F_Q and F_P are the components of R normal to and parallel to the cutting direction, and $\beta = \tan^{-1} F_C/N_C$ (is called the friction angle).

Assuming the shear stress on the shear plane (τ) to be uniformly distributed it is evident that

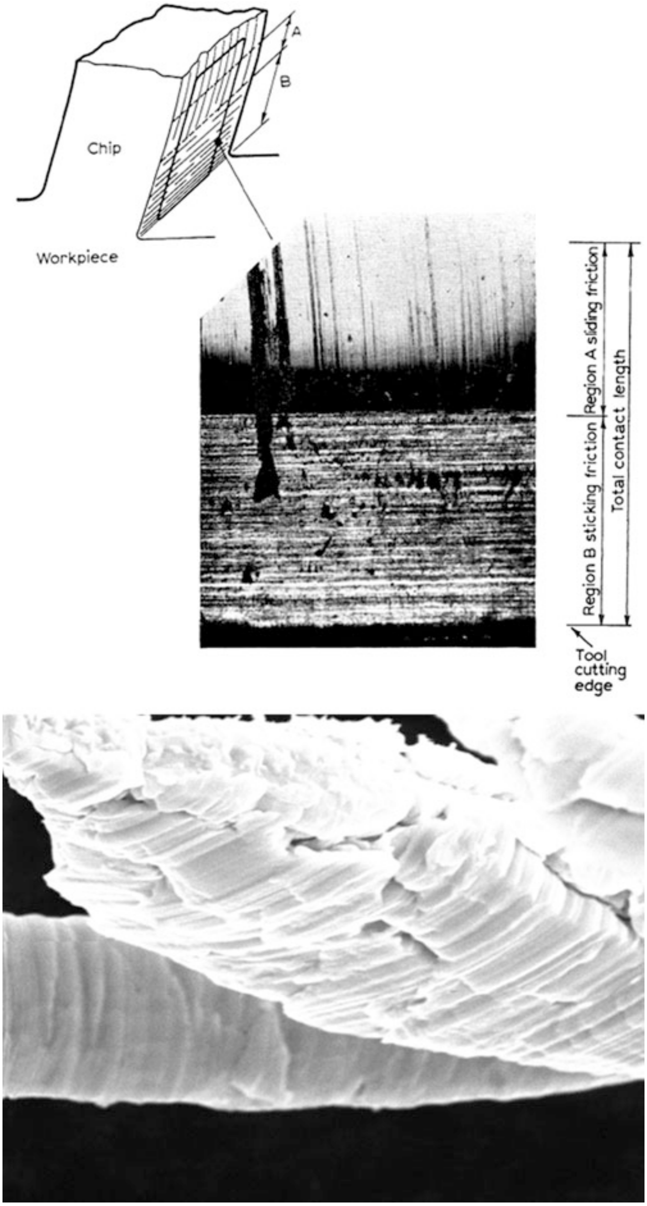

Fig. 1.5 Back free surface of a quick-stop and a free chip showing regions of discontinuous strain or microfracture [3]

Fig. 1.6 Nomenclature for two-dimensional steady-state orthogonal cutting process [5]

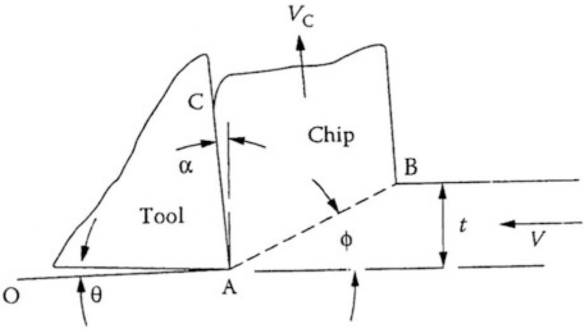

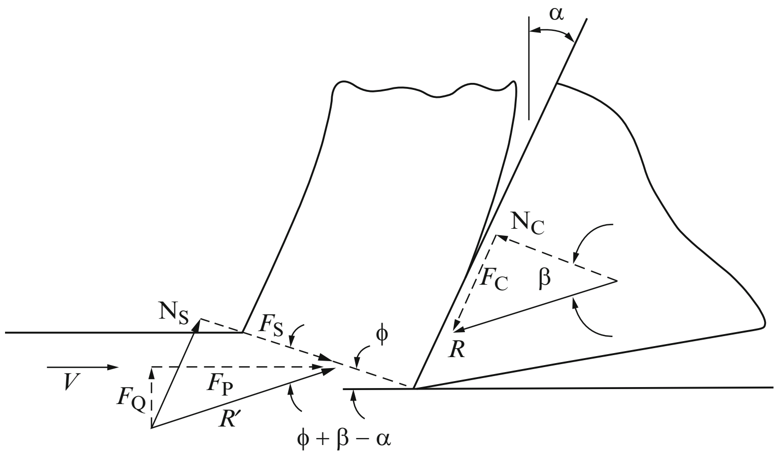

Fig. 1.7 Cutting forces at the tool tip for the cutting operation shown in Fig. 1.6 [5]

$$\tau = \frac{F_S}{A_S} = \frac{R' \cos(\phi + \beta - \alpha) \sin \phi}{A} \tag{1.1}$$

where A_S and A are the areas of the shear plane and that corresponding to the width of cut (b), times the depth of cut (t). Ernst and Merchant [5] reasoned that τ should be an angle such that τ would be a maximum and a relationship for ϕ was obtained by differentiating (1.1) with respect to ϕ and equating the resulting expression to zero produces

$$\phi = 45 - \frac{\beta}{2} + \frac{\alpha}{2} \tag{1.2}$$

However, it is to be noted that in differentiating, both R' and β were considered independent of ϕ.

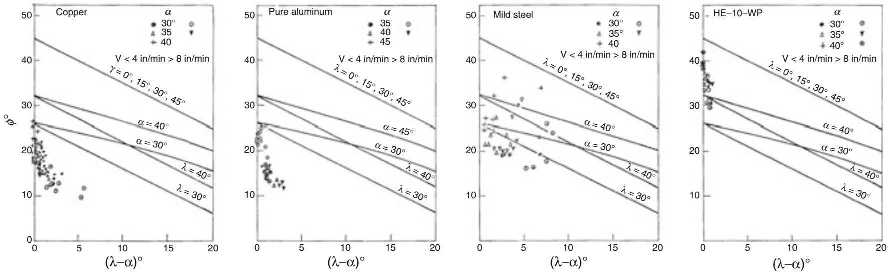

Fig. 1.8 Relationship between ϕ and $(\lambda - \alpha)$ for various workpiece materials (After Pugh given in [3])

Merchant [6] presented a different derivation that also led to (1.2). This time an expression for the total power consumed in the cutting process was first written as

$$P = F_P V = (\tau A V) \frac{\cos(\beta - \alpha)}{\sin\phi \cos(\phi + \beta - \alpha)} \tag{1.3}$$

It was then reasoned that ϕ would be such that the total power would be a minimum. An expression identical to (1.2) was obtained when P was differentiated with respect to ϕ, this time considering τ and β to be independent of ϕ. The Merchant relationship is shown in Fig. 1.8 for a selection of workpiece materials.

Piispanen [7] had done this previously in a graphical way. However, he immediately carried his line of reasoning one step further and assumed that the shear stress τ would be influenced directly by normal stress on the shear plane as follows:

$$\tau = \tau_0 + K_\sigma \tag{1.4}$$

where K is a material constant. Piispanen then incorporated this into his graphical solution for the shear angle. Upon finding (1.2) to be in poor agreement with experimental data Merchant also independently (without knowledge of Piispanen's work at the time) assumed that the relationship given in (1.4), and proceeded to work this into his second analysis as follows. From Fig. 1.7 it may be seen that

$$\sigma = \tau \tan(\phi + \beta - \alpha) \tag{1.5}$$

or from (1.4)

$$\tau_0 = \tau + K\tau \tan(\phi + \beta - \alpha) \tag{1.6}$$

Hence,

$$\tau = \frac{\tau_0}{1 - K \tan(\phi + \beta - \alpha)} \tag{1.7}$$

Table 1.1 Values of C in (1.9) for a variety of work and tool materials in finish turning without a cutting fluid

Work material	Tool material	C (Degrees)
SAE 1035 Steel	HSS[a]	70
SAE 1035 Steel	Carbide	73
SAE 1035 Steel	Diamond	86
AISI 1022 (leaded)	HSS[a]	77
AISI 1022 (leaded)	Carbide	75
AISI 1113 (sul.)	HSS[a]	76
AISI 1113 (sul.)	Carbide	75
AISI 1019 (plain)	HSS[a]	75
AISI 1019 (plain)	Carbide	79
Aluminum	HSS[a]	83
Aluminum	Carbide	84
Aluminum	Diamond	90
Copper	HSS[a]	49
Copper	Carbide	47
Copper	Diamond	64
Brass	Diamond	74

[a] *HSS* high-speed steel

When this is substituted into (1.3), we have

$$P = \frac{\tau_0 AV \cos(\beta - \alpha)}{[1 - K \tan(\phi + \beta - \alpha)] \sin\phi \cos(\phi + \beta - \alpha)} \quad (1.8)$$

Now, when P is differentiated with respect to ϕ and equated to zero (with τ_0 and p considered independent of ϕ), we obtain

$$\phi = \frac{\cot^{-1}(K)}{2} - \frac{\beta}{2} + \frac{\alpha}{2} = \frac{C - \beta + \alpha}{2} \quad (1.9)$$

Merchant called the quantity, $\cot^{-1} K$, the machining "constant" C. The quantity C is seen to be the angle the assumed line relating τ and ϕ makes with the τ axis [6–8]. Merchant [9] has determined the values of C given in Table 1.1 for materials of different chemistry and structure being turned under finishing conditions with different tool materials. From this table it is evident that C is not a constant. Merchant's empirical machining "constant" C that gives rise to (1.9) with values of ϕ is in reasonably good agreement with experimentally measured values.

While it is well established that the rupture stress of both brittle and ductile materials is increased significantly by the presence of compressive stress (known as the Mohr Effect), it is generally believed that a similar relationship for flow stress does not hold. However, an explanation for this paradox with considerable supporting experimental data is presented below. The fact that this discussion is limited to steady-state chip formation rules out the possibility of periodic gross cracks being involved. However, the role of microcracks is a possibility consistent with steady-state chip formation and the influence of compressive stress on the flow stress in shear.

A discussion of the role microcracks can play in steady-state chip formation is presented in the next section. Hydrostatic stress plays no role in the plastic flow of metals if they have no porosity. Yielding then occurs when the von Mises criterion reaches a critical value. Merchant [8] has indicated that Barrett [10] found that for single crystal metals τ_S is independent of φ_S when plastics such as celluloid are cut. In general, if a small amount of compressibility is involved yielding will occur when the von Mises criterion reaches a certain value.

However, based on the results of Table 1.1, the role of compressive stress on shear stress on the shear plane in steady-state metal cutting is substantial. The fact there is no outward sign of voids or porosity in steady-state chip formation of a ductile metal during cutting and yet there is a substantial influence of normal stress on shear stress on the shear plane represents an interesting paradox. It is interesting to note that Piispanen [7] had assumed that shear stress on the shear plane would increase with normal stress and had incorporated this into his graphical treatment.

1.1.2 Plastic Behavior at Large Strains

There has been little work done in the region of large plastic strains. Bridgman [11] used hollow tubular notched specimens to perform experiments under combined axial compression and torsion. Strain was concentrated in the reduced sections and it was possible to crudely estimate and plot shear stress vs. shear strain with different amounts of compressive stress on the shear plane. From these experiments Bridgman concluded that the flow curve for a given material was the same for all values of compressive stress on the shear plane, a result consistent with other materials experiments involving much lower plastic strains. However, the strain at gross fracture was found to be influenced by compressive stress. A number of related results and size effect models are considered in the following subsections.

1.1.3 Langford and Cohen's Model

Langford and Cohen [12] were interested in the behavior of dislocations at very large plastic strains and whether there was saturation relative to the strain-hardening effect with strain, or whether strain hardening continued to occur with strain to the point of fracture. Their experimental approach was an interesting and fortunate one. They performed wire drawing on iron specimens using a large number of progressively smaller dies with remarkably low semi die angle (1.5°)

and a relatively low (10 %) reduction in area per die pass. After each die pass, a specimen was tested in uniaxial tension and a true stress–strain curve obtained. The drawing and tensile experiments were performed at room temperature and low speeds to avoid heating and specimens were stored in liquid nitrogen between experiments to avoid strain aging effects. All tensile results were then plotted in a single diagram, the strain used being that introduced in drawing (0.13 per die pass) plus the plastic strain in the tensile test. The general overlap of the tensile stress–strain curves gives an overall strain-hardening envelope, which indicates that the wire drawing and tensile deformations are approximately equivalent relative to strain hardening [13].

Blazynski and Cole [14] were interested in strain hardening in tube drawing and tube sinking. Drawn tubes were sectioned and tested in plane strain compression. Up to a strain of about 1 the usual strain-hardening curve was obtained that is in good agreement with the generally accepted equation,

$$\sigma = \sigma_1 \varepsilon^n \tag{1.10}$$

However, beyond a strain of 1, the curve was linear corresponding to the equation,

$$\sigma = A + B\varepsilon, \quad (\varepsilon < 1) \tag{1.11}$$

where A and B are constants. It may be shown that

$$A = (1 - n)\sigma_1 \tag{1.12}$$

$$B = n\sigma_1 \tag{1.13}$$

From transmission electron micrographs of deformed specimens, Langford and Cohen found that cell walls representing concentrations of dislocations began to form at strains below 0.2 and became ribbon shaped with decreasing mean linear intercept cell size as the strain progressed. Dynamic recovery and cell wall migration resulted in only about 7 % of the original cells remaining after a strain of 6. The flow stress of the cold-worked wires was found to vary linearly with the reciprocal of the mean transverse cell size [15].

1.1.4 Walker and Shaw's Model

Acoustic studies were performed on specimens of the Bridgman type but fortunately, lower levels of axial compressive stress than Bridgman had used were employed in order to more closely simulate the concentrated shear process of metal cutting. The apparatus used that was capable of measuring stresses and strains as well as acoustic signals arising from plastic flow is described in the dissertation of Walker [16]. Two important results were obtained:

1. A region of rather intense acoustical activity occurred at the yield point followed by a quieter region until a shear strain of about 1.5 was reached. At this point there was a rather abrupt increase in acoustical activity that continued to the strain at fracture which was appreciably greater than 1.5.
2. The shear stress appeared to reach a maximum at strain corresponding to the beginning of the second acoustic activity ($\gamma \approx 1.5$).

The presence of the notches in the Bridgman specimen made interpretation of stress–strain results somewhat uncertain. Therefore, a new specimen was designed which substitutes simple shear for torsion with normal stress on the shear plane. By empirically adjusting distance Δx to a value of 0.25 mm it was possible to confine all the plastic shear strain to the reduced area, thus making it possible to readily determine the shear strain ($\gamma \approx \Delta y / \Delta x$). When the width of minimum section was greater or less than 0.25 mm, the extent of plastic strain observed in a transverse micrograph at the minimum section either did not extend completely across the 0.25 mm dimension or beyond this width.

Similar results were obtained for non-resulfurized steels and other ductile metals. There is little difference in the curves for different values of normal stress on the shear plane (σ) to a shear strain of about 1.5 [17]. This is in agreement with Bridgman. However, beyond this strain the curves differ substantially with compressive stress on the shear plane. At large strains, τ was found to decrease with increase in (γ), a result that does not agree with Bridgman [11].

It is seen that for a low value of normal stress on the shear plane of 40 MPa strain hardening appears to be negative at a shear strain of about 1.5; that is, when the normal stress on the shear plane is about 10 % of the maximum shear stress reached, negative strain hardening sets in at a shear strain of about 1.5. On the other hand, strain hardening remains positive to a normal strain of about 8 when the normal stress on the shear plane is about equal to the maximum shear stress.

1.1.5 Usui's Model

In Usui et al. [18] an experiment is described designed to determine why CCl_4 is such an effective cutting fluid at low cutting speeds. Since this also has a bearing on the role of microcracks in large strain deformation, it is considered here. A piece of copper was prepared [18]. The piece that extends upward and appears to be a chip is not a chip but a piece of undeformed material left there when the specimen was prepared. A vertical flat tool was then placed precisely opposite the free surface and fed horizontally. Horizontal F_P and vertical F_Q forces were recorded as the shear test proceeded. It was expected that the vertical piece would fall free from the lower material after the vertical region had been displaced a small percentage of its length. However, it went well beyond the original extent of the shear plane and was still firmly attached to the base. This represents a huge shear strain since the shear deformation was confined to a narrow band. When a single drop of CCl_4 was placed

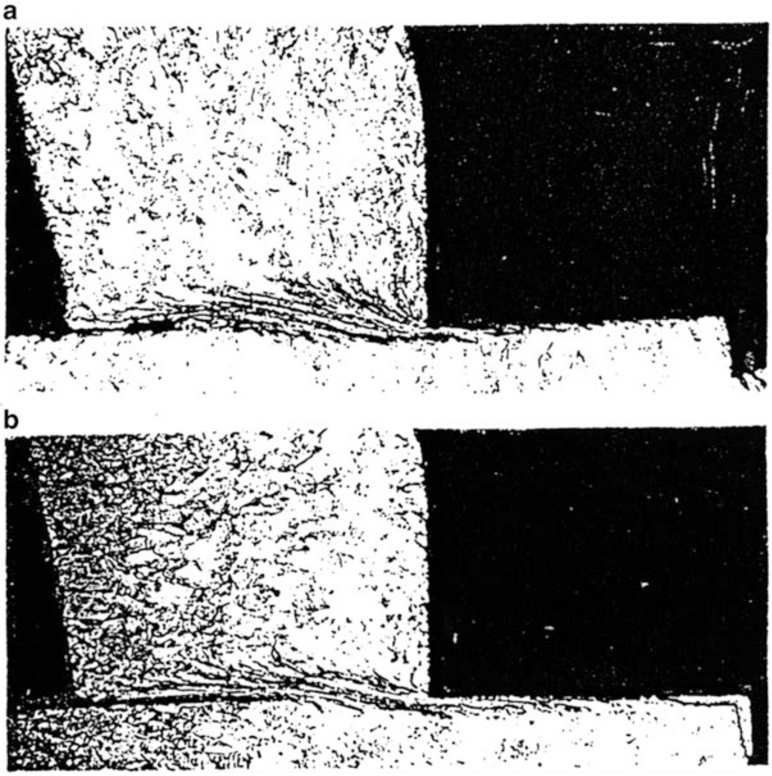

Fig. 1.9 Photomicrographs of specimens that have been sheared a distance approximately equal to the shear plane length: (**a**) in air and (**b**) with a drop of CCl_4 applied [3]

before the shear test was conducted, the protrusion could be moved only a fraction of the displacement in air before gross fracture occurred on the shear plane. Figure 1.9 shows photomicrographs of experiments without and with CCl_4. It is apparent that CCl_4 is much more effective than air in preventing microcracks from re-welding.

1.1.6 Saw Tooth Chip Formation

Saw tooth chip formation for hard steel discussed by Vyas and Shaw [19] is another example of the role microcracks play. In this case gross cracks periodically form at the free surface and run down along the shear plane until sufficient compressive stress is encountered to cause the gross crack to change to a collection of isolated microcracks.

1.1.7 Fluid-Like Flow in Chip Formation

An interesting paper was presented by Eugene [20]. Water was pumped into baffled chamber that removed eddy currents and then caused flow under gravity past a simulated tool. Powdered bakelite was introduced to make the streamlines visible as the fluid flowed passed the tool.

The photographs taken by the camera were remarkably similar to quick stop photomicrographs of actual chips. It was thought by this author at the time that any similarity between fluid flow and plastic flow of a solid was not to be expected. That was long before it was clear that the only logical explanation for the results of Bridgman and Merchant involve microfracture [21]. A more recent paper was presented that again suggests that metal cutting might be modeled by a fluid [22]. However, this paper was concerned with ultraprecision machining (depths of cut <4 μm) and potential flow analysis was employed instead of the experimental approach taken by Eugene.

It is interesting to note that chemists relate the flow of liquids to the migration of vacancies (voids) just as physicists relate ordinary plastic flow of solid metals to the migration of dislocations. Henry Eyring and co-workers [23–25] have studied the marked changes in volume, entropy, and fluidity that occur when a solid melts. For example, a 12 % increase in volume accompanies melting of Argon, suggesting the removal of every eighth molecule as a vacancy upon melting. This is consistent with X-ray diffraction of liquid argon that showed good short-range order but poor long-range order. The relative ease of diffusion of these vacancies accounts for the increased fluidity that accompanies melting.

A random distribution of vacancies is also consistent with the increase in entropy observed on melting. Eyring's theory of fluid flow was initially termed the *hole theory of fluid flow* but later *The Significant Structure Theory* which is the title of the Eyring-Jhon book [24]. According to this theory, the vacancies in a liquid move through a sea of molecules. Eyring's theory of liquid flow is mentioned here since it explains why the flow of a liquid approximates the flow of metal passed a tool in chip formation. In this case microcracks (voids) move through a sea of crystalline solid.

1.2 Size Effects in Micromachining

It is appropriate at this point to mention that an alternative explanation for the increase in hardness that occurs when the indentation size is reduced in metals has recently been introduced [26–37]. This is based on the fact that there is an increase in the strain gradient with reduction in indentation size. This has been extended by Dinesh et al. [38] to explain the size effect in machining. In the Dinesh et al. [38] analysis the size effect in hardness is related to that in cutting by assuming the von

Mises criterion is applicable. Based on the experiments of Merchant, it is evident that this is not applicable in steady-state chip formation.

In this strain gradient theory two types of dislocations are proposed: geometrically necessary dislocations (ρ_g) that are responsible for work hardening and statistically stored dislocations (ρ_S) that are affected by a strain gradient. When $\rho_g \gg \rho_S$ conventional plasticity pertains (strain rate unimportant) but when $\rho_g \ll \rho_S$ a constitutive equation including strain rate should be included.

The impression one obtains in reading Dinesh et al. [38] is that the strain gradient approach is uniquely responsible for the size effect in cutting. In their concluding remarks it is suggested that it should be possible to verify the validity of the strain rate formulation by experiments designed to test predictions of this approach. This has not yet been done and until it is it will not be possible to determine whether the influence of strain rate is significant in the chip formation application. In any case, it is believed the explanation presented here based on the influence of defects and normal stress on the shear plane is sufficiently well supported by the experiments described that it should not be considered insignificant.

1.3 Nanomachining

Nanomachining can be classified into four categories:

- Deterministic mechanical nanometric machining. This method utilizes fixed and controlled tools, which can specify the profiles of three-dimensional components by a well-defined tool surface and path. The method can remove materials in amounts as small as tens of nanometers. It includes typically diamond turning, micromilling, and nano/microgrinding.
- Loose abrasive nanometric machining. This method uses loose abrasive grits to remove a small amount of materials. It consists of polishing, lapping, and honing.
- Nonmechanical nanometric machining. It comprises focused ion beam machining, micro-EDM, and excimer laser machining.
- Lithographic method. It employs masks to specify the shape of the product. Two-dimensional shapes are the main outcome; severe limitations occur when three-dimensional products are attempted. It mainly includes X-ray lithography, LIGA, electron beam lithography.

Mechanical nanometric machining has more advantages than other methods since it is capable of machining complex 3D components in a controllable way. The machining of complex surface geometry is just one of the future trends in nanometric machining, which is driven by the integration of multiple functions in one product.

For instance, the method can be used to machine micromoulds and dies with complex geometric features and high dimensional and form accuracy, and even nanometric surface features. The method is indispensable to manufacturing complex micro- and miniature structures, components and products in a variety of engineering materials. This chapter focuses on nanometric cutting theory, methods and its implementation and application perspectives [39–43].

1.3.1 Nanometric Machining

Single-point diamond turning and ultraprecision grinding are two major nanometric machining approaches. They are both capable of producing extremely fine cuts. Single-point diamond turning has been widely used to machine nonferrous metals such as aluminum and copper. An undeformed chip thickness about 1 nm is observed in diamond turning of electroplated copper [44]. Diamond grinding is an important process for the machining of brittle materials such as glasses and ceramics to achieve nanometer levels of tolerances and surface finish. A repeatable optical quality surface roughness (surface finish <10 nm Ra) has been obtained in nanogrinding of hard steel by Stephenson et al. using 76 μm grit cBN wheel on the ultra-precision grinding machine tool [45]. Recently, diamond fly-cutting and diamond milling have been developed for machining non-rotational non-symmetric geometry, which has enlarged the product spectrum of nanometric machining [46]. In addition the utilization of ultra-fine grain hard metal tools and diamond coated microtools represents a promising alternative for microcutting of even hardened steel [47].

Early applications of nanometric machining are in the mass production of some high precision parts for microproducts, or microsystems. In fact, microproducts, or microsystems, will be the first path that enables nanoproducts to enter the marketplace since microproducts, or microsystems, have been dominating nanotechnology application markets worldwide [48]. It also anticipates that microproducts will have more and more requirements around the world. It is very interesting to see that the IT peripheral market is still the biggest market of microproducts. In 2005, the total turnover of microproducts reached US$38 billion, which is two times that of the total turnover in 2000. Nanometric machining can be applied in bulk machining of silicon, aluminum substrates for computer memory disks, etc. In other areas such as biomedical, automotive, household, and telecommunication the total turnovers of microproducts are still steadily growing. Nanometric machining is also very promising in the production of sensors, accelerometer, actuators, micro-mirror, fiber optics connectors, and micro-displays. In fact applications of nanoproducts will enhance the performance of microproducts in the form of sensitivity, selectivity, and stability [49]. In 2006, IT lost this predominant position owing to new MEMS-based applications in sectors such as biotechnology and communication (optical and radio frequency switching, for example, will become a major growth area) [50]. Nanometric machining still has priority in this application area. The microproducts are normally integrated products of some electronics, mechanical parts and optical parts while in miniature or microdimensions. In fact only small number of microproducts solely relies on electronics. The mechanical and optical parts are of significant importance for microproducts. The indispensable advantage of nanometric machining is its applicability to manufacture 3D complex components/devices including micromoulds, dies, and embossing tooling for cheap mass production of optical and mechanical parts. Therefore, it is undoubtedly one of the major enabling technologies for commercialization of nanotechnology in the future.

1.3.2 Theoretical Basis of Nanomachining

Scientific study of nanometric machining has been undertaken since late 1990s. Much attention to the study has been paid especially with the advance of nanotechnology [51]. The scientific study will result in the formation of the theoretical basis of nanometric machining, which enables the better understanding of nanometric machining physics and the development of its controllable techniques to meet the advanced requirements for nanotechnology and nanoscience.

1.3.2.1 Cutting Force and Energy

In nanomanufacturing, the cutting force and cutting energy are important issues. They are important physical parameters for understanding cutting phenomena as they clearly reflect the chip removal process. From the aspect of atomic structures cutting forces are the superposition of the interactions forces between workpiece atoms and cutting tool atoms. Specific energy is an intensive quantity that characterizes the cutting resistance offered by a material [52].

Ikawa et al. and Luo et al. have acquired the cutting forces and cutting energy by molecular dynamics simulations [51–54]. Moriwaki and Lucca have carried out experiments to measure the cutting forces in nanometric machining [51]. Figure 1.10 shows the simulation and experimental results in nanometric cutting. Figure 1.10a illustrates the linear relation exists between the cutting forces per width and depth of uncut in both simulations and experiments. The cutting forces per width increase with the increment of the depth of cut.

The difference in the cutting force between the simulations and the experiments is caused by the different cutting edge radii applied in the simulations. In nanometric machining the cutting edge radius plays an important role since the depth of cut is similar in scale. Under the same depth of cut higher cutting forces are needed for a tool with a large cutting edge radius compared with a tool with a small cutting edge radius.

The low cutting force per width is obviously the result of fine cutting conditions, which will decrease the vibration of the cutting system and thus improve the machining stability and will also result in better surface roughness. A linear relationship between the specific energy and the depth of cut can also be observed

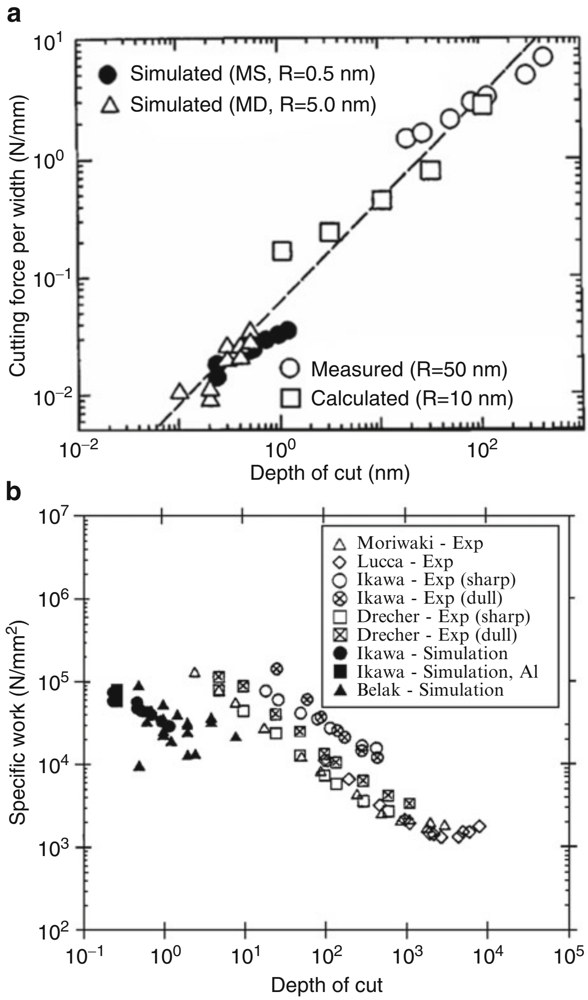

Fig. 1.10 Comparison of results between simulations and experiments: (**a**) cutting force per width against depth of cut; (**b**) specific energy against depth of cut [51]

in Fig. 1.10b. The figure shows that the specific energy increases with a decreasing of depth of cut, because the effective rake angle is different under different depths of cut. In small depths of cut the effective rake angle will increase with the decreasing of depth of cut. Large rake angle results in the increasing of specific energy.

This phenomenon is often called the "size effect," which can be clearly explained by material data listed in Table 1.2. According to Table 1.2, in nanometric machining only point defects exist in the machining zone in a crystal, so it will need more energy to initiate the atomic-crack or atomic-dislocation. The decreasing of depth of cut will decrease the chance for the cutting tool to meet point defects and result in the increasing of the specific cutting energy.